agronomy

MDPI

Article

Potassium Fulvate Alleviates Salinity and Boosts Oat Productivity by Modifying Soil Properties and Rhizosphere Microbial Communities in the Saline–Alkali Soils of the Qaidam Basin

Jie Wang [1], Xin Jin [1], Xinyue Liu [1], Yunjie Fu [2], Kui Bao [2], Zhixiu Quan [2], Chengti Xu [3,4,5], Wei Wang [3,4,5], Guangxin Lu [1,*] and Haijuan Zhang [6,*]

1 College of Agriculture and Animal Husbandry, Qinghai University, Xining 810016, China; wangjie422022@163.com (J.W.); 18894310895@163.com (X.J.); 17856838703@163.com (X.L.)
2 Qinghai Bensheng Grass Industry Co., Ltd., Delingha 817000, China; fszyjr@126.com (Y.F.); 13141752025@163.com (K.B.); 258800qzx@sina.com (Z.Q.)
3 Northwest Key Laboratory of Cultivated Land Conservation and Marginal Land Improvement, Ministry of Agriculture and Rural Affairs, Delingha 817000, China; xchti@163.com (C.X.); 13997194054@163.com (W.W.)
4 Academy of Animal Science and Veterinary Medicine, Qinghai University, Xining 810003, China
5 National Grass Varieties Regional Test Station, Delingha 817000, China
6 Key Laboratory of Plateau Climate Change and Its Eco-Environmental Effects, Qinghai Institute of Technology, Xining 810016, China
* Correspondence: lugx74@163.com (G.L.); 15297196583@163.com (H.Z.); Tel.: +86-13897216290 (G.L.); +86-15509714323 (H.Z.)

Abstract

Soil salinization severely limits global agricultural sustainability, particularly across the saline–alkaline landscapes of the Qinghai–Tibet Plateau. We examined how potassium fulvate (PF) modulates oat (*Avena sativa* L.) performance, soil chemistry, and rhizospheric microbiota in the saline–alkaline soils of the Qaidam Basin. PF markedly boosted shoot and root biomass, with the greatest response observed at 150 kg hm^{-2}. At the same time, it enhanced soil fertility by increasing organic matter, nitrate-N, ammonium-N, and available potassium, and improved ionic balance by lowering Na^+ concentrations and the sodium adsorption ratio (SAR), while increasing Ca^{2+} levels and soil moisture content. Under the high-dose treatment (F2), endogenous fungal contributions declined sharply, exogenous replacements increased, and fungal α-diversity fell; multivariate ordinations confirmed that PF reshaped both bacterial and fungal communities, with fungi exhibiting the stronger response. We integrated three machine learning algorithms—least absolute shrinkage and selection operator (LASSO), Random Forest (RF), and eXtreme Gradient Boosting (XGBoost)—to minimize the bias inherent in any single method. We identified microbial β-diversity, organic matter, and Na^+ and Ca^{2+} concentrations as the most robust predictors of the Soil Salinization and Alkalization Index (SSAI). Structural equation modeling further showed that PF mitigates salinity chiefly by improving soil physicochemical properties (path coefficient = -0.77; $p < 0.001$), with microbial assemblages acting as key intermediaries. These findings provide compelling theoretical and empirical support for deploying PF to rehabilitate saline–alkaline soils in alpine environments and offer practical guidance for sustainable land management in the Qaidam Basin.

Keywords: sustainable soil management; Soil Salinization and Alkalization Index; machine-learning; Qaidam Basin

check for updates

Academic Editor: Kenneth J. Moore

Received: 9 June 2025
Revised: 1 July 2025
Accepted: 9 July 2025
Published: 10 July 2025

Citation: Wang, J.; Jin, X.; Liu, X.; Fu, Y.; Bao, K.; Quan, Z.; Xu, C.; Wang, W.; Lu, G.; Zhang, H. Potassium Fulvate Alleviates Salinity and Boosts Oat Productivity by Modifying Soil Properties and Rhizosphere Microbial Communities in the Saline–Alkali Soils of the Qaidam Basin. *Agronomy* **2025**, *15*, 1673. https://doi.org/10.3390/agronomy15071673

Copyright: © 2025 by the authors. Licensee MDPI, Basel, Switzerland. This article is an open access article distributed under the terms and conditions of the Creative Commons Attribution (CC BY) license (https://creativecommons.org/licenses/by/4.0/).

1. Introduction

Soil salinization and alkalization represents one of the most pressing global environmental challenges, affecting nearly 1×10^9 ha, which accounts for approximately 33.3% of the Earth's land surface [1]. Compared with other regions, China is particularly affected, with salt-affected soils covering 3.47×10^7 ha, approximately 3.5% of the global estimate [2]. The impact of salinity stress is especially acute in the arid regions of Northwest China, where low precipitation and high evaporation severely hinder crop growth and limit agricultural productivity [3,4]. On the Qinghai–Tibetan Plateau, particularly in the Qaidam Basin, harsh climatic conditions such as low temperatures, drought, and severe salt accumulation severely constrain the development of the local forage industry and hinder the sustainable utilization of land resources [5,6].

Contemporary saline land management strategies typically rely on hydrological interventions to reduce surface salinity and improve soil structure by flushing accumulated salts from the root zone through integrated irrigation and drainage systems [7,8]. Precise control of irrigation volume and drainage timing helps to suppress excessive evaporation and upward salt migration, thereby significantly reducing salt concentrations in the root zone [9,10]. However, frequent irrigation and drainage can lead to nutrient leaching and destabilize soil ecological functions [11,12]. In the Qaidam Basin, where precipitation is minimal and water availability is limited, the effectiveness of hydrological measures is substantially constrained, often resulting in the reaccumulation of surface salts [13,14].

Phytoremediation is a cost-effective and environmentally sustainable strategy for alleviating soil salinity, relying on stress-adapted plant species to extract or redistribute excess ions and thereby enhance the long-term viability of agricultural land [15,16]. In the Qaidam Basin, oat (*Avena sativa* L.) has been identified as a key forage crop due to its exceptional tolerance to salinity, low temperatures, and drought. Its high yield potential under these conditions has been consistently demonstrated in multiple field studies [17,18].

Conventional chemical treatments for salt-affected soils often involve the use of amendments such as gypsum, aluminum sulfate, or ferrous sulfate to regulate ion exchange and pH, and to reduce soluble salt load [15,19–21], thereby improving overall soil chemical stability and structure. In recent years, potassium fulvate (PF), a promising organic amendment, has attracted growing interest. PF can directly mitigate ionic stress by modifying soil chemistry [22,23], and indirectly promote plant resilience by enhancing root architecture and nutrient use efficiency [24,25]. PF has also been shown to restructure microbial communities and restore key soil ecological functions [26–28]. However, its potential to improve soil quality, support vegetation growth, and regulate rhizosphere microbial dynamics in the salt-affected soils of the Qaidam Basin remains largely unexamined.

Given the widespread distribution of saline–alkaline soils and limited precipitation in the Qaidam Basin, it is particularly necessary to develop a soil remediation strategy that integrates potassium fulvate (PF) application with the cultivation of a stress-adapted oat variety. In this study, field experiments were conducted in saline–alkaline agricultural areas of the Qaidam Basin on the Qinghai–Tibetan Plateau. The locally adapted and widely cultivated oat cultivar 'Qingtian No. 1' (*Avena sativa* L.) was used as the test crop under three treatments: a no-fertilizer control (CK) and two PF application rates (F1: 75 kg·hm^{-2}, F2: 150 kg·hm^{-2}). This study specifically proposed the following hypotheses: (i) PF application promotes oat growth; (ii) PF improves rhizosphere soil conditions under saline–alkaline stress; (iii) PF regulates rhizosphere microbial community structure; and (iv) PF alleviates saline–alkaline soil constraints by jointly modifying soil physicochemical properties and microbial assemblages. By systematically testing these hypotheses, this research aims to provide a solid theoretical framework and practical basis for PF application in saline–alkaline regions of the Qinghai–Tibetan Plateau, offering scientific guidance and

new approaches for the sustainable development and utilization of saline–alkaline land in the Qaidam Basin.

2. Materials and Methods

2.1. Experimental Site

This study was conducted in the Qaidam Basin, Qinghai Province, China (37°22′38.784″ N, 97°43′58.962″ E; 3158 m; Figure 1). The site lies within a high-elevation desert fringe of the Qinghai–Tibet Plateau and is characterized by arid, windy conditions, low atmospheric oxygen, and scant precipitation, resulting in an extremely fragile ecosystem [28,29]. In the Chinese Soil Taxonomy, the surface layer is identified as plateau saline soil [30]; correspondingly, the World Reference Base for Soil Resources (IUSS Working Group WRB, 2022) places soils with a salic horizon within the upper 50 cm in the Reference Soil Group Solonchak [31]. Prior to sowing, saturated paste extract electrical conductivity (ECe) in the 0–30 cm layer averaged 4.73 dS m^{-1}, surpassing the FAO diagnostic threshold of 4 dS m^{-1} for saline soils [32,33].

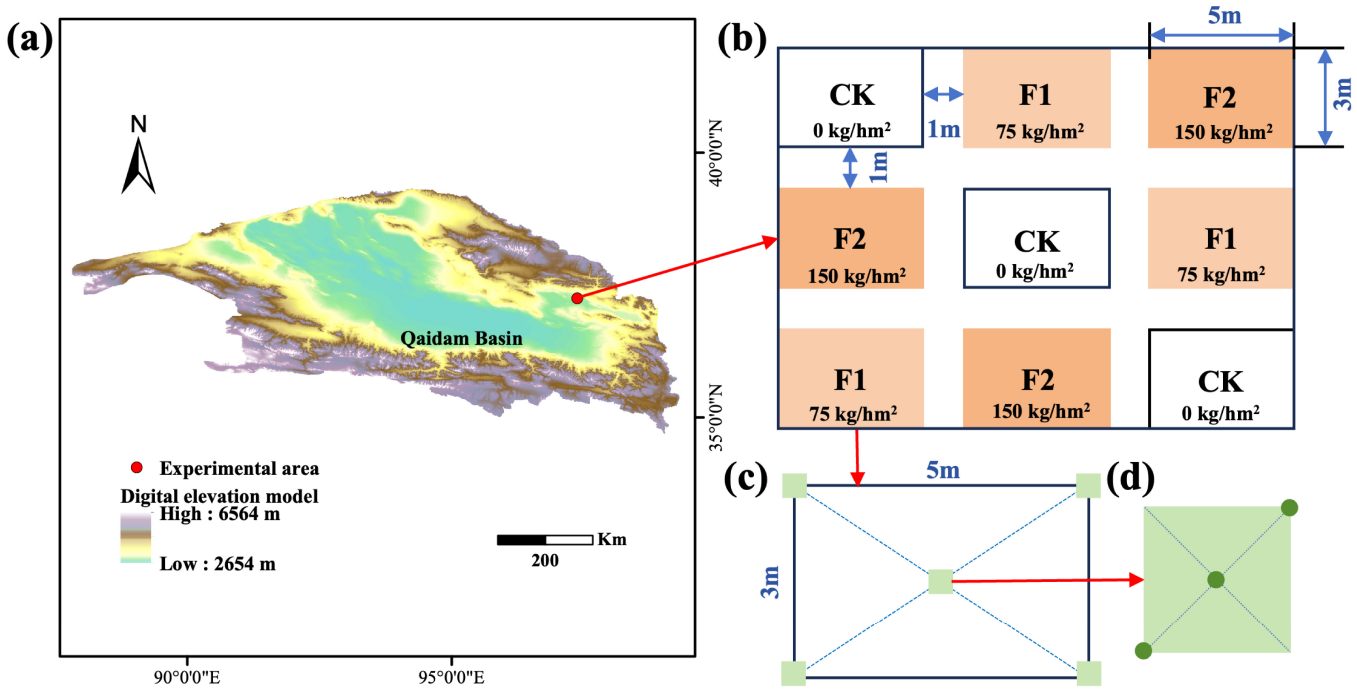


Figure 1. Study site, experimental layout, and rhizosphere soil sampling workflow. (**a**) Geographic location of the Qaidam Basin field site on the Qinghai–Tibet Plateau. (**b**) Arrangement of potassium-fulvate experimental plots. (**c**) Arrangement of five 1 m × 1 m quadrats within each 5 m × 3 m plot. (**d**) Schematic of a single quadrat showing the three rhizosphere-soil sampling points: two vertices on the same diagonal and the center. Note: Basemap data in panel (**a**) sourced from the National Cryosphere Desert Data Center (http://www.ncdc.ac.cn, accessed on 1 April 2023). CK, untreated control; F1, potassium fulvate 75 kg hm^{-2}; F2, potassium fulvate 150 kg hm^{-2}.

2.2. Experimental Materials and Design

The field trial began on 4 May 2023. Certified oat 'Qingtian No. 1' (90% germination, >90% purity; Qinghai Kairui Ecological Technology Co., Ltd.) seed was sown at 300 kg hm^{-2}. Potassium fulvate (PF), supplied by Jining Jinshan Bioengineering Co., Ltd. (Jining, China) and containing 11% K_2O, 4% N, and 68% organic matter (*w*/*w*), was employed as an amendment. Before sowing, 300 kg hm^{-2} of a granular sheep manure compost (organic matter: 45%, total N: 1.8%, P_2O_5: 1.2%, K_2O: 1.1%; Qinghai Shuanghe Organic Fertilizer Co., Ltd., Delingha, China) and 375 kg hm^{-2} of compound fertilizer (N:P_2O_5:K_2O = 25:12:5, Qinghai Shuanghe Organic Fertilizer Co., Ltd., Delingha, China) were incorporated.

A Latin square design was used with three treatments, each replicated three times (nine plots): CK (no PF), F1 (75 kg hm^{-2} PF), and F2 (150 kg hm^{-2} PF). Each 5 m × 3 m plot was separated by a 1 m buffer. The seeds were hand-sown in 3–4 cm-deep furrows, 30 cm apart, with PF thoroughly mixed into the sowing furrow. All plots were irrigated uniformly three times per month with sprinkler-applied groundwater (20 mm per event), ensuring that soil moisture in the 0–20 cm layer did not fall below 60% of field capacity. The plot layout is shown in Figure 1. The preceding crop was oat (*Avena sativa* L., cv. 'Qingtian No. 1'). The surface soil (0–30 cm) was classified as saline-calcic, at pH 8.5–9.2; the baseline physicochemical properties are listed in Figure 2.

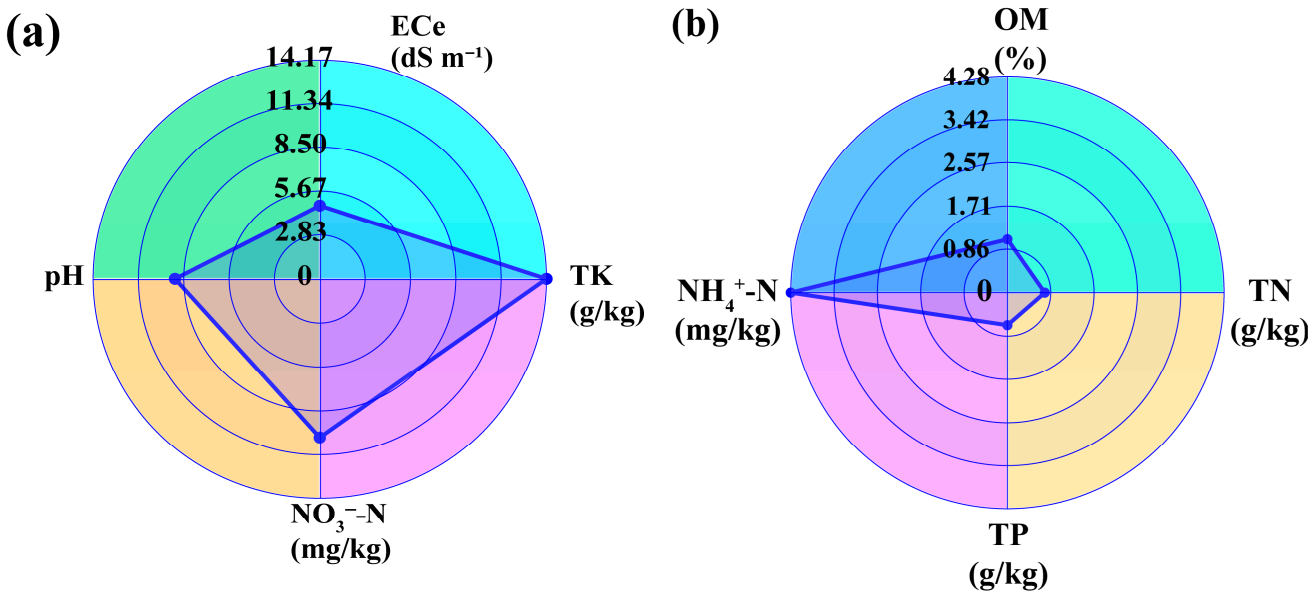


Figure 2. Initial physicochemical characteristics of the topsoil before sowing. (**a**) Soil pH, nitrate-nitrogen (NO_3^-–N), and total potassium (TK); (**b**) organic matter (OM), ammonium–nitrogen (NH_4^+–N), total nitrogen (TN), and total phosphorus (TP). Note: All measurements refer to the 0–30 cm soil layer at the experimental site.

2.3. Soil Sampling for Chemical and Microbiological Studies

At maturity, when more than 85% of the panicles had turned yellow, five locations were chosen along each plot's diagonal, and three soil cores (0–15 cm depth, 38 mm diameter) were collected at each location. Bulk soil was gently shaken off; tightly adhering rhizosphere soil was brushed into sterile bags for physicochemical assays. Intact roots with attached rhizosphere soil were sealed in sterile bags, chilled at −20 °C during transport, and stored at −80 °C.

For rhizosphere extraction, roots were vortexed and sonicated three times in 30 mL sterile PBS (pH 7.0, 0.1% Tween-80). Combined suspensions were centrifuged (6000 rpm, 5 min); pellets were freeze-dried (−40 °C, ≥12 h) and kept at −80 °C for DNA extraction.

2.4. Plant and Soil Measurements

The heights of thirty uniform plants per plot were measured to a precision of 0.01 cm. Six 50 cm row segments per plot were harvested; aboveground biomass and belowground biomass were weighed fresh, oven-dried (105 °C for 30 min followed by 65 °C to constant mass), and their dry weights were recorded for subsequent data analysis. From the harvested material, ten plants per plot were randomly chosen for root morphology analysis. Root morphology (length, surface area, volume) was quantified on ten roots per

plot using an Epson V700 scanner and WinRhizo Pro 2016 (Perfection V700 Photo; Seiko Epson Corporation, Suwa, Nagano, Japan).

Soil pH (1:2.5 soil:water) was measured with a PHS-3C meter; electrical conductivity and moisture (0–10 cm) were measured with a TDR-350 sensor. Total N and P were determined by semi-micro Kjeldahl and continuous-flow molybdate methods, respectively [34]. Organic matter was analyzed via dichromate oxidation [35]; NO_3^-–N and NH_4^+–N were analyzed by UV spectrophotometry and indophenol colorimetry [36]. Total K was measured after digestion by atomic fluorescence spectrometry; K^+ was measured by flame photometry [37]. Air-dried soil (<2 mm) was wetted to saturation and equilibrated 4 h, and the saturated paste was vacuum-filtered to obtain the extract (1 mL g^{-1}). Soluble Na^+, Ca^{2+}, and Mg^{2+} were quantified in the filtrate by ICP-OES (ICP-OES; Optima 8300, PerkinElmer Inc., Waltham, MA, USA) with a 0–100 mg L^{-1} multi-element calibration ($R^2 \geq 0.999$). A blank, a duplicate, and the certified soil GBW07456 were inserted every ten samples [38].

2.5. DNA Extraction and Sequencing

Genomic DNA was extracted from 0.25 g rhizosphere soil. The bacterial 16S-V4 region (primers 515F/806R) and fungal ITS2 region (5.8F/4R) were amplified by 25-cycle FastPfu PCR (55 °C annealing). Amplicons were purified, pooled equimolarly, and sequenced (PE250) on an Illumina MiSeq.

Reads were demultiplexed, quality-filtered (≥50 bp), merged (≥10 bp overlap, ≤20% mismatch), chimera-checked, and denoised to amplicon sequence variants. The data were rarefied to 30,159 (16S) and 46,591 (ITS) reads per sample for subsequent analyses.

2.6. Statistical Analysis

Normality was assessed with the Shapiro–Wilk test and variance homogeneity with the Levene test. Variables that met both assumptions—belowground biomass (BGB), total biomass (TB), root length, root volume, NO_3^-–N, NH_4^+–N, exchangeable Na^+, soil moisture content (SMC), sodium adsorption ratio (SAR), bacterial richness, Pielou evenness, β-diversity, habitat niche breadth (HNB), and the corresponding fungal metrics (richness, Shannon diversity, Pielou evenness, phylogenetic diversity, β-diversity, habitat niche breadth)—were analyzed with one-way ANOVA; significant F-tests ($\alpha = 0.05$) were followed by Bonferroni-adjusted pairwise comparisons. Variables that failed any assumption—aboveground biomass (AGB), root surface area, organic matter (OM), total phosphorus (TP), total nitrogen (TN), available K, exchangeable Mg^{2+} and Ca^{2+}, pH, electrical conductivity (EC), bacterial Shannon diversity, bacterial phylogenetic diversity, and fungal β-diversity—were evaluated with the Kruskal–Wallis test, and significant results were parsed with Dunn–Bonferroni post hoc tests [39–41].

The FEAST algorithm was employed to perform microbial source tracking across CK, F1, and F2 treatments, enabling rapid and accurate quantification of source contributions for each microbial group and revealing treatment-specific patterns of community turnover [42]. Microbial α-diversity metrics, including richness, Pielou's evenness, Shannon diversity, and phylogenetic diversity, were analyzed using one-way ANOVA followed by Bonferroni-adjusted multiple comparisons [43]. Principal coordinate analysis (PCoA) was conducted to visualize shifts in microbial community structure across treatments [44]. To further confirm group separations, partial least squares discriminant analysis (PLS-DA) was performed as a complementary approach [45]. The statistical significance of community differences among treatments was assessed using permutational multivariate analysis of variance (PERMANOVA) and analysis of similarity (ANOSIM), with Bonferroni-adjusted *p*-values applied to correct for multiple comparisons [46].

Soil sodium adsorption ratio (SAR), defined as the molar ratio of Na^+ to (Ca^{2+} + Mg^{2+}), is widely used to gauge sodicity; larger values denote greater salinity–alkalinity risk [47]. To obtain a single diagnostic metric, we constructed a Soil Salinization and Alkalization Index (SSAI) that integrates SAR, soil pH, and electrical conductivity (EC) [48]. SSAI is a dimensionless, entropy-weighted metric that captures the combined effects of osmotic, sodic, and alkaline stress in Qaidam soils, without reintroducing the saline sodic category. Because all three variables increase with salinity–alkalinity intensity, each was first standardized by Z-score transformation to remove scale effects [49,50]. Objective weights for the standardized variables were then derived with the entropy-weight method [51], which assigns higher weights to parameters exhibiting greater information entropy (dispersion). SSAI was calculated as the weighted sum of the three normalized indices [52]; higher SSAI values therefore indicate more severe soil salinization and alkalization.

Because conventional linear regression cannot capture the nonlinear and high-order interactions that underlie variation in the Soil Salinization and Alkalization Index (SSAI), we adopted a multi-algorithm machine learning framework [53]. All predictors, except for SAR, soil pH, and electrical conductivity (EC), which were used to define SSAI, were Z-score standardized and subsequently screened using three complementary embedded methods. (i) Least Absolute Shrinkage and Selection Operator (LASSO) regression, implemented with ten-fold cross-validation, was used to obtain a parsimonious feature set; predictors whose coefficients remained non-zero at the optimal penalty parameter (λ_min) were retained [54]. (ii) Random forest (100 trees, nodesize = 2) ranked variables by minimal node depth, an index of how early a predictor is selected to split the trees; variables with average depths $\leq$ the forest mean were retained, thereby capturing nonlinear and interaction effects [55]. (iii) XGBoost (objective = "reg:squarederror", η = 0.1, nrounds = 100) evaluated predictor importance by gain and retained the top 20 features [56]. Feature sets from the three algorithms were intersected with ggvenn; variables common to all sets were designated robust predictors of the SSAI. The workflow relies on the R packages glmnet, randomForestSRC, xgboost, ggvenn, and ggplot2.

The variables common to LASSO, Random Forest, and XGBoost were taken as the robust predictors of the Soil Salinization and Alkalization Index (SSAI) [57]. These predictors, along with the potassium fulvate dose, were entered into a partial least squares structural equation model (PLS-SEM) implemented in the plspm package to trace the pathway from PF through key predictors to the SSAI. Model adequacy was judged with the global goodness-of-fit statistic (GOF); values above 0.33 were considered acceptable [58,59]. All statistical analyses and figure visualizations were performed with R version 4.4.1.

3. Results

3.1. Effects of Potassium Fulvate Application on Oat Growth

Under saline–alkaline soil conditions in the Qaidam Basin, the application of potassium fulvate (PF) significantly enhanced oat biomass accumulation. Both F1 (75 kg·hm^{-2}) and F2 (150 kg·hm^{-2}) treatments markedly increased belowground biomass (BGB) and total biomass (TB), with F2 producing the most pronounced effect ($p < 0.01$; Figure 3a). Aboveground biomass (AGB) also increased significantly under F2 compared with the CK ($p < 0.01$; Figure 3a), suggesting that applying PF at a higher rate is more effective in stimulating shoot growth. Additionally, both F1 and F2 significantly increased root surface area and volume ($p < 0.05$; Figure 3b). Although differences in root length were not statistically significant, the average values in plots receiving PF were higher than those in the control. These findings indicate that PF application, particularly at increased levels, enhances root system architecture and thereby contributes to improved overall biomass production.

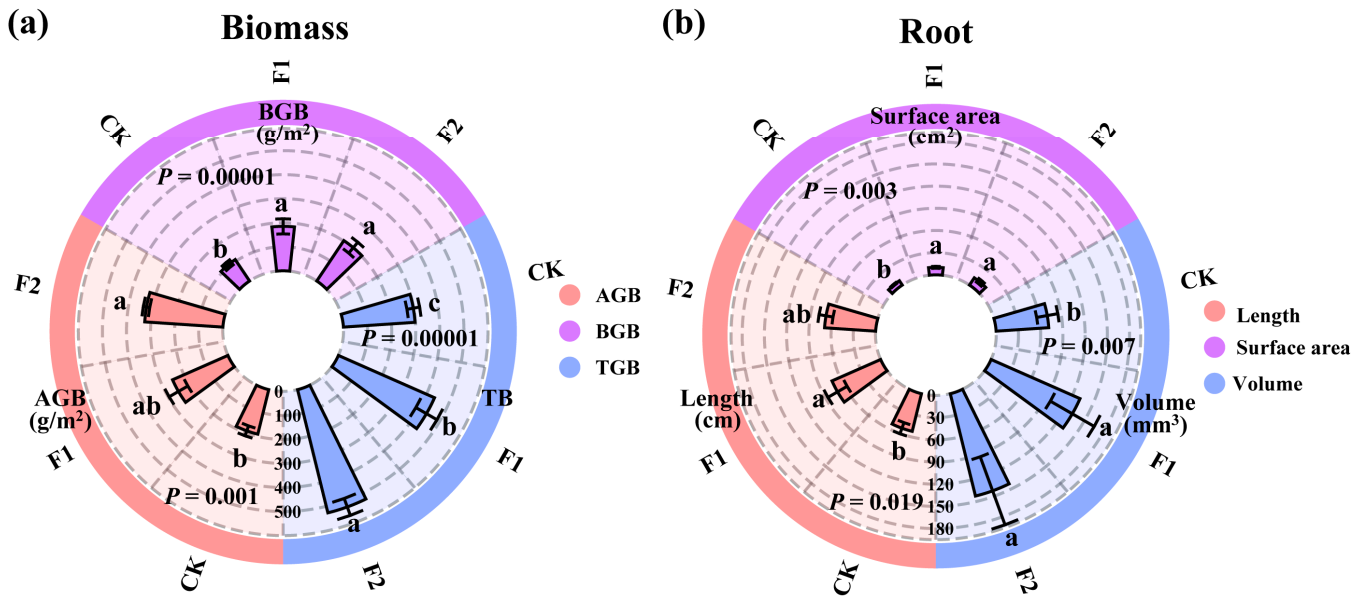


Figure 3. Potassium fulvate enhances oat biomass accumulation and root morphology. (**a**) Responses of aboveground biomass (AGB), belowground biomass (BGB), and total biomass (TB). (**b**) Effects on root morphological traits. Note: Aboveground biomass (AGB); belowground biomass (BGB); total biomass (TB). Note: Different lowercase letters indicate significant differences among treatments. CK, untreated control; F1, potassium fulvate 75 kg hm^{-2}; F2, potassium fulvate 150 kg hm^{-2} (n = 6 per treatment).

3.2. Effects of Potassium Fulvate Application on Rhizosphere Soil

Application of potassium fulvate (PF) significantly improved the physicochemical properties of oat rhizosphere soil (Figure 4a–f). Relative to the control (CK), both PF application rates led to significant increases in soil organic matter (OM), nitrate nitrogen (NO_3^-–N), and total potassium (TK) ($p < 0.01$; Figure 4a,d,f), with the greatest enhancement in OM observed under the higher rate (F2). Ammonium nitrogen (NH_4^+–N) also exhibited an upward trend under both F1 and F2 applications, and the increase in F2 was significantly greater than in CK ($p < 0.05$; Figure 4e), although the difference between F1 and F2 was not statistically significant. In contrast, total phosphorus (TP) and total nitrogen (TN) concentrations were not significantly altered ($p > 0.05$; Figure 4b,c), suggesting that PF had a limited effect on the accumulation of bulk nutrients.

Potassium fulvate (PF) application significantly influenced the ionic composition and physicochemical properties of oat rhizosphere soil under saline–alkaline conditions. Compared with the control (CK), both PF application levels (F1 and F2) resulted in notable reductions in soil sodium (Na^+) concentrations and sodium adsorption ratio (SAR) ($p < 0.01$; Figure 5a,d), with the F2 treatment exerting a stronger effect, underscoring its capacity to alleviate sodium-induced stress. Calcium ion (Ca^{2+}) levels were significantly elevated under F2 ($p < 0.01$; Figure 5c), while magnesium ion (Mg^{2+}) concentrations remained statistically unchanged across treatments. Soil pH and electrical conductivity (EC) both declined following PF addition, with the lowest values observed in F2 ($p < 0.01$; Figure 5e,f), suggesting a mitigation of salinity-related impacts. Moreover, soil moisture content (SMC) increased significantly in the F2 group ($p < 0.001$; Figure 5g), indicating enhanced water retention capacity. Overall, potassium fulvate contributed to a more favorable rhizosphere soil environment by lowering Na^+ and SAR, raising Ca^{2+} availability, reducing salinity indicators such as pH and EC, and improving soil moisture status, with the higher application level yielding the most substantial improvements.

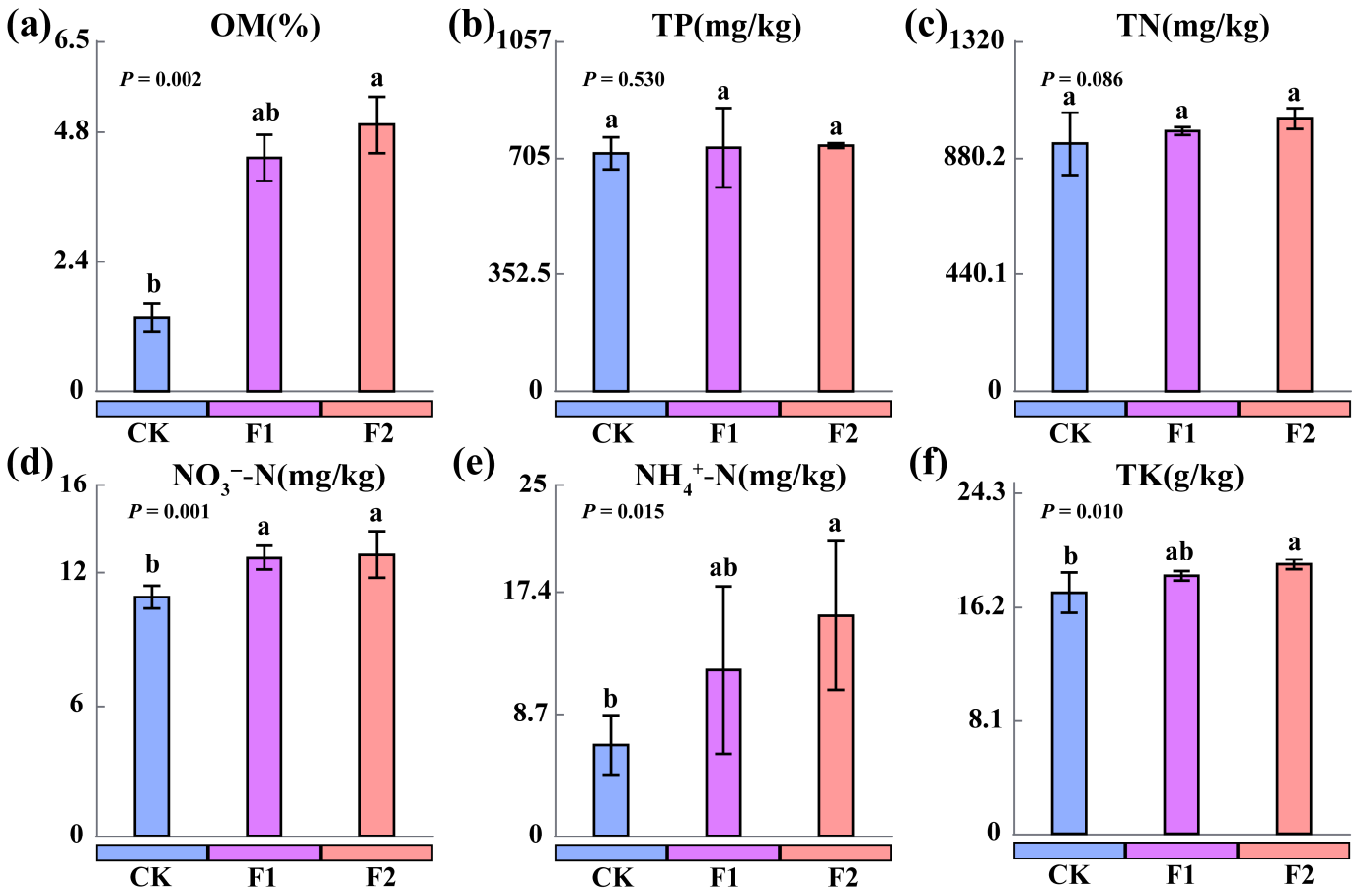


Figure 4. Potassium fulvate effects on soil nutrients. (**a**) Organic matter (OM); (**b**) total phosphorus (TP); (**c**) total nitrogen (TN); (**d**) nitrate–nitrogen (NO_3^-–N); (**e**) ammonium–nitrogen (NH_4^+–N); (**f**) total potassium (TK). Note: Different lowercase letters indicate significant differences among treatments. CK, untreated control; F1, potassium fulvate 75 kg hm^{-2}; F2, potassium fulvate 150 kg hm^{-2} (n = 6 per treatment).

3.3. Effects of Potassium Fulvate Application on Rhizosphere Microorganisms

To investigate how potassium fulvate (PF) application influences the origins of rhizosphere microbial communities, microbial source tracking was conducted using the FEAST algorithm, with bacterial and fungal communities analyzed separately. In the bacterial community, F1 and F2 were mainly derived from the control (CK), with source contributions of 62.05% and 52.44%, respectively, and a 62.18% shared origin between the two treatments (Figure 6a). These findings suggest that PF application resulted in relatively stable bacterial community composition, with limited turnover. In contrast, the fungal community exhibited higher sensitivity to PF application. While 56.16% of F1 originated from CK, the contribution from CK to F2 declined to 35.78%. Notably, F1 accounted for 44.97% of the F2 fungal community (Figure 6b). These results indicate that higher PF application intensified fungal community turnover and facilitated compositional restructuring.

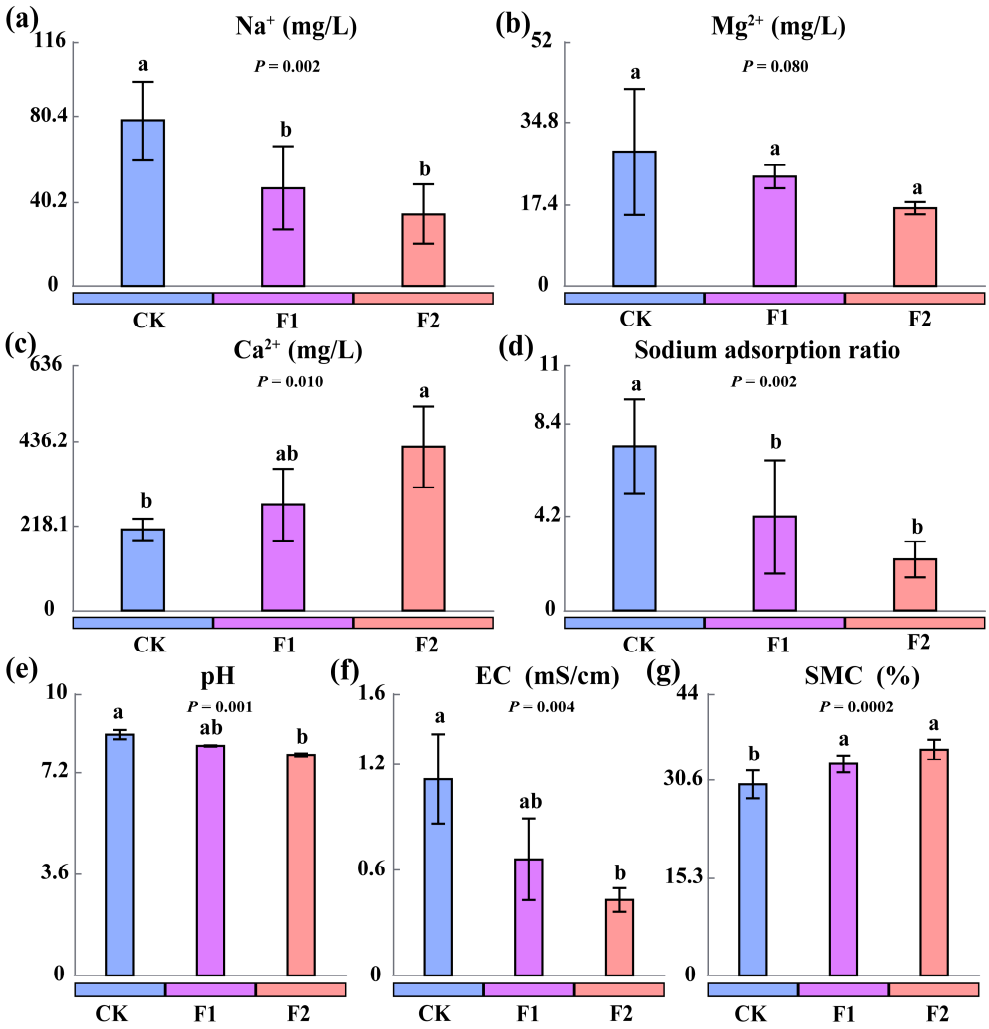


Figure 5. Potassium fulvate effects on soil physicochemical properties. (**a**) Sodium ion (Na^+); (**b**) magnesium ion (Mg^{2+}); (**c**) calcium ion (Ca^{2+}); (**d**) sodium adsorption ratio (SAR); (**e**) soil pH; (**f**) electrical conductivity (EC); (**g**) soil moisture content (SMC). Note: Different lowercase letters indicate significant differences among treatments. CK, untreated control; F1, potassium fulvate 75 kg hm^{-2}; F2, potassium fulvate 150 kg hm^{-2} (n = 6 per treatment).

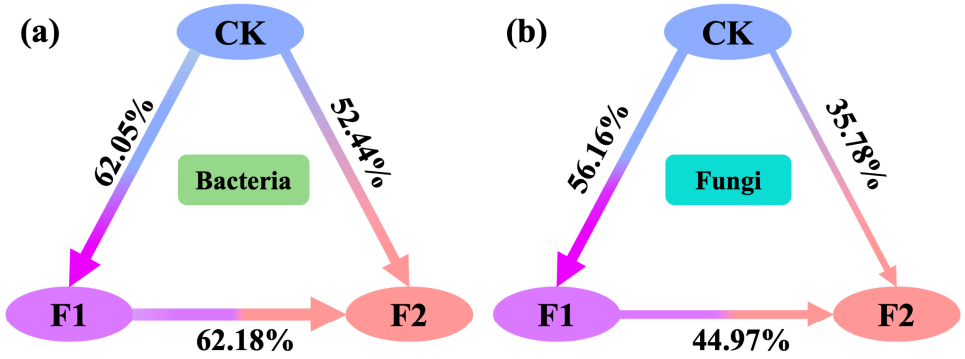


Figure 6. Potassium fulvate reshapes rhizosphere microbial source–sink patterns. (**a**) Source contributions to bacterial communities under CK, F1, and F2 treatments; (**b**) source contributions to fungal communities under CK, F1, and F2 treatments. Note: Source-tracking was performed with FEAST. Arrows originate from source communities and terminate at sink communities; arrow width is proportional to relative contribution. CK, untreated control; F1 (75 kg hm^{-2} PF), and F2 (150 kg hm^{-2} PF).

Regarding rhizosphere microbial α-diversity, potassium fulvate (PF) exerted minimal influence on bacterial communities. No significant differences were observed across treatments in species richness, Shannon diversity, Pielou evenness, or phylogenetic diversity ($p > 0.05$; Figure 7a–d), indicating compositional stability under PF application. In contrast, the fungal community exhibited a distinct dose-dependent response (Figure 7e–h). Significant declines were observed in species richness ($p < 0.001$; Figure 7e), Shannon index ($p < 0.01$; Figure 7f), Pielou evenness ($p < 0.05$; Figure 7g), and phylogenetic diversity ($p < 0.001$; Figure 7h) under the high-dose F2 treatment. In summary, PF exerted a progressively suppressive effect on fungal α-diversity, whereas its influence on bacterial diversity remained negligible.

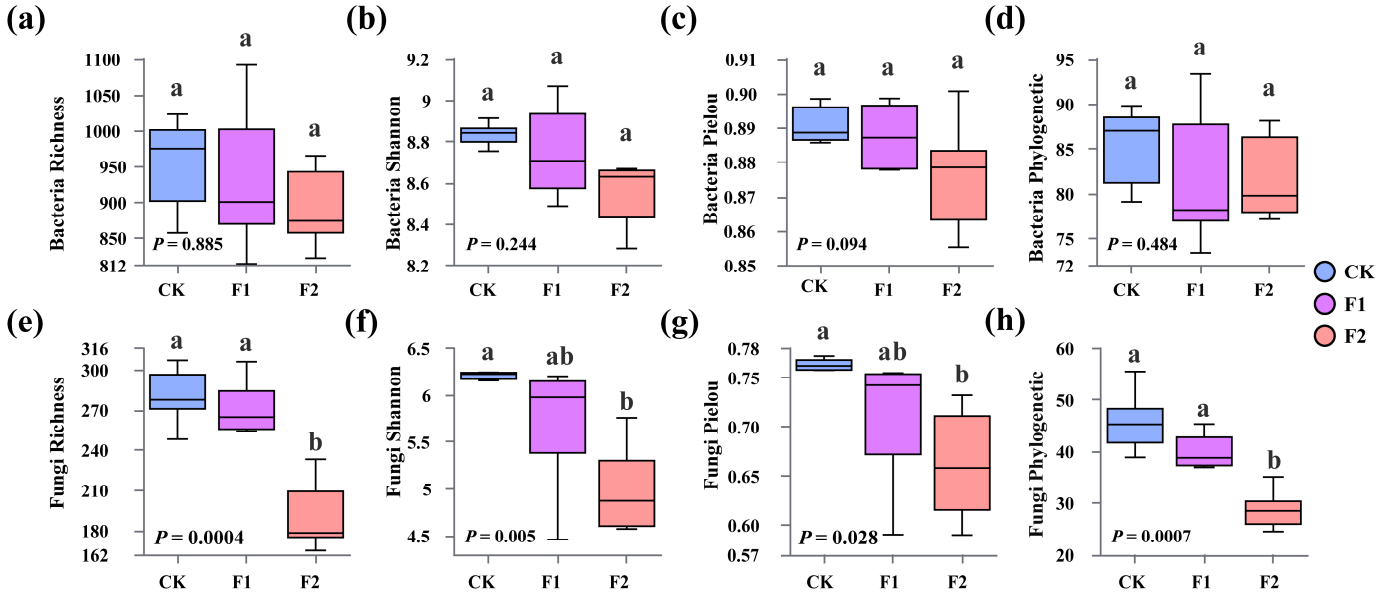


Figure 7. Effects of potassium fulvate on the α-diversity of rhizosphere microbial communities. (**a**–**d**) rhizosphere soil bacterial communities; (**e**–**h**) rhizosphere soil fungal communities. Note: Different lowercase letters indicate significant differences among treatments. CK, untreated control; F1, potassium fulvate 75 kg hm^{-2}; F2, potassium fulvate 150 kg hm^{-2} (n = 6 per treatment).

To assess the impact of potassium fulvate (PF) application on oat rhizosphere microbial composition, both bacterial and fungal communities were examined using Principal Coordinate Analysis (PCoA) and partial least squares discriminant analysis (PLS-DA). PCoA revealed distinct separation of both F1 and F2 treatments from the control (CK) in bacterial (Figure 8a) and fungal (Figure 8b) community structures. These differences were supported by PERMANOVA analysis ($p < 0.01$). Notably, the F2 treatment exhibited the greatest divergence, indicating a stronger influence of high-dose FAP on microbial restructuring. PLS-DA further corroborated these findings. In the bacterial community, the three treatments were distinctly clustered (Figure 8c), and ANOSIM confirmed significant group differences ($p < 0.01$; Figure 8c). A similar pattern was observed for fungi, with a marked distinction between F2 and CK ($p < 0.01$; Figure 8d). In summary, PF application substantially altered rhizosphere microbial community composition, with the high-dose F2 treatment inducing pronounced restructuring, particularly in fungal communities.

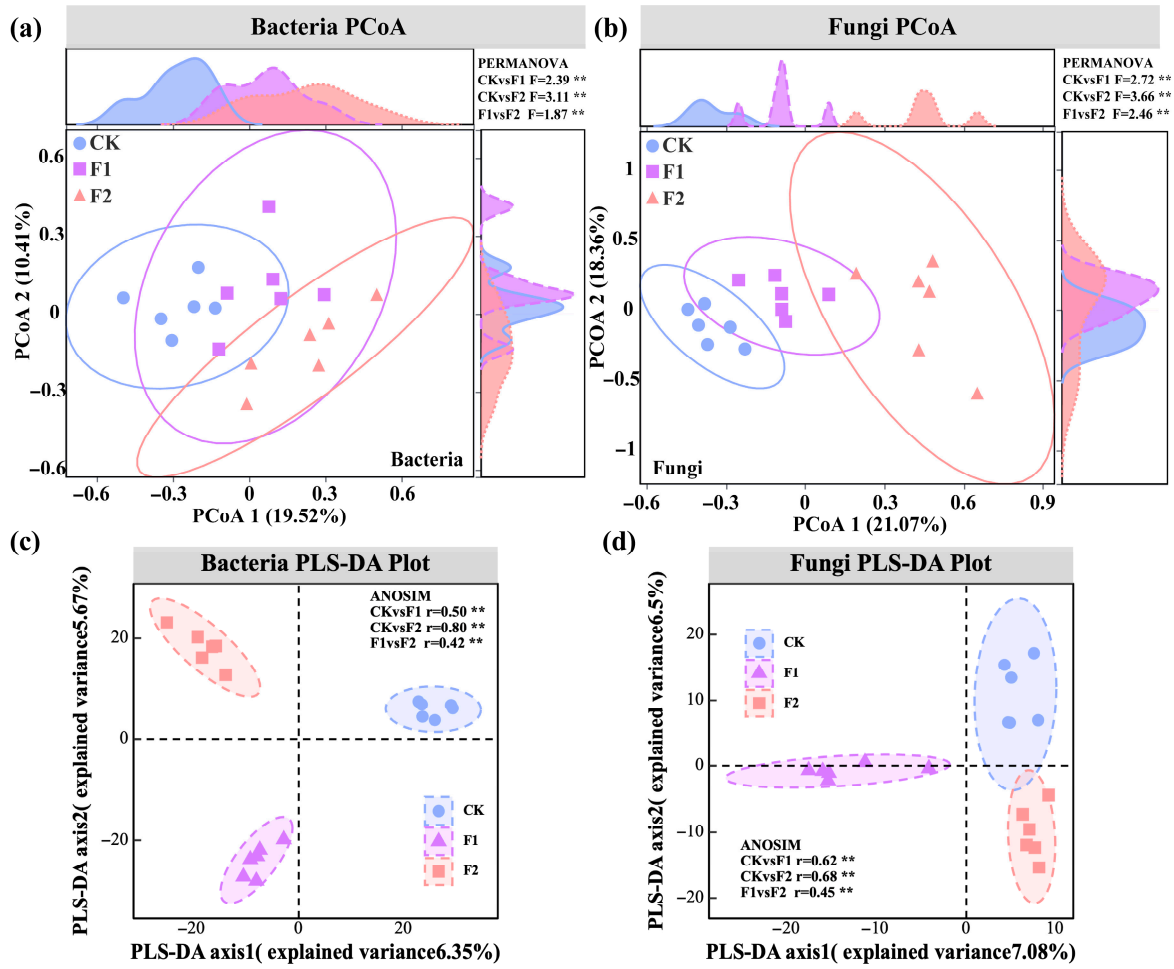


Figure 8. Potassium fulvate reshapes rhizosphere microbial community structure. (**a**) Principal coordinates analysis (PCoA) of bacterial communities (PERMANOVA, ** $p < 0.01$). (**b**) Principal coordinates analysis (PCoA) of fungal communities (PERMANOVA, ** $p < 0.01$). (**c**) Partial least squares discriminant analysis (PLS-DA) of bacterial communities (ANOSIM, ** $p < 0.01$). (**d**) PLS-DA of fungal communities (ANOSIM, ** $p < 0.01$). Note: CK, untreated control; F1, potassium fulvate 75 kg hm^{-2}; F2, potassium fulvate 150 kg hm^{-2} (n = 6 per treatment).

The application of potassium fulvate (PF) was found to influence the niche breadth of rhizosphere microbial communities. In bacterial communities, HNB values did not differ significantly among treatments ($p > 0.05$; Figure 9), indicating a minimal impact of FP on bacterial niche breadth. By contrast, fungal communities appeared to be more sensitive to FP application ($p < 0.05$; Figure 9). Compared to the control (CK), the F1 treatment significantly broadened fungal niche breadth ($p < 0.05$; Figure 9), while the F2 treatment led to a marked compression of HNB values ($p < 0.05$; Figure 9). These results indicate that high-dose FP may contribute to niche compression in fungal communities.

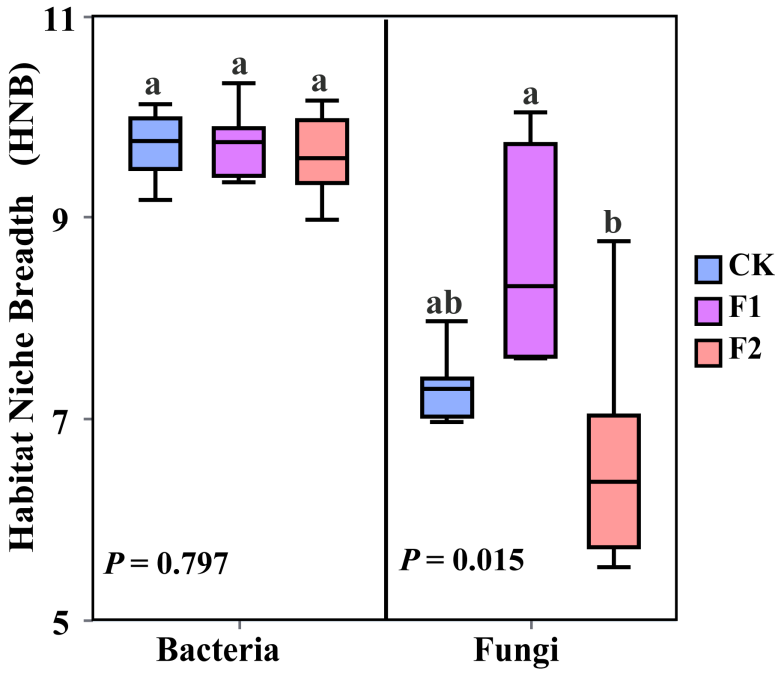


Figure 9. Effects of potassium fulvate on the habitat niche breadth of rhizosphere microbial communities. Note: Different lowercase letters indicate significant differences among treatments. CK, untreated control; F1, potassium fulvate 75 kg hm^{-2}; F2, potassium fulvate 150 kg hm^{-2} (n = 6 per treatment).

3.4. Effects of Potassium Fulvate Application on Rhizosphere Soil Salinity and Alkalinity

A quantification of rhizospheric salt–alkaline stress was achieved through the development of a comprehensive index called the Soil Salinization and Alkalization Index (SSAI), which incorporates soil sodium adsorption ratio (SAR), pH, and electrical conductivity (EC) to capture the extent of salinity–alkalinity stress in the rhizosphere. The results showed that the application of potassium fulvate (PF) significantly reduced SSAI values ($p < 0.001$; Figure 10a). Both F1 and F2 treatments exhibited significantly lower SSAI values compared to the control (CK) ($p < 0.001$; Figure 10a), and the F2 treatment resulted in the most pronounced reduction, suggesting that PF effectively alleviates rhizospheric salinity–alkalinity stress, particularly when applied at higher rates.

Aiming to determine the key factors influencing SSAI, we employed three machine learning methods, namely LASSO regression, Random Forest, and XGBoost, for systematic feature selection (Figure S1). LASSO regression (Figure 10b) identified the fungal Pielou index, various fungal diversity metrics, organic matter (OM), and sodium ions (Na^+) as the primary contributing factors. Random Forest (Figure 10c) and XGBoost (Figure 10d) confirmed the importance of OM, Na^+, the fungal Pielou index, and microbial diversity traits in explaining SSAI variability. Robustness was ensured by identifying overlapping variables that were selected by all three methods (Figure 10e). The results showed that bacterial β-diversity, fungal β-diversity, the fungal Pielou index, OM, Na^+, and Ca^{2+} were consistently identified as core predictors and serve as reliable indicators for predicting soil salinization–alkalization status.

Further elucidation of the mechanisms by which potassium fulvate (PF) mitigates rhizospheric salinization–alkalization via microbial–soil interactions was achieved using a partial least squares structural equation model (PLS-SEM). This model integrated PF application, microbial communities, soil physicochemical properties, and the Soil Salinization and Alkalization Index (SSAI). The SEM showed a strong overall fit (GOF = 0.82) and accounted for 93% of the variation in SSAI ($R^2 = 0.93$; Figure 11a).

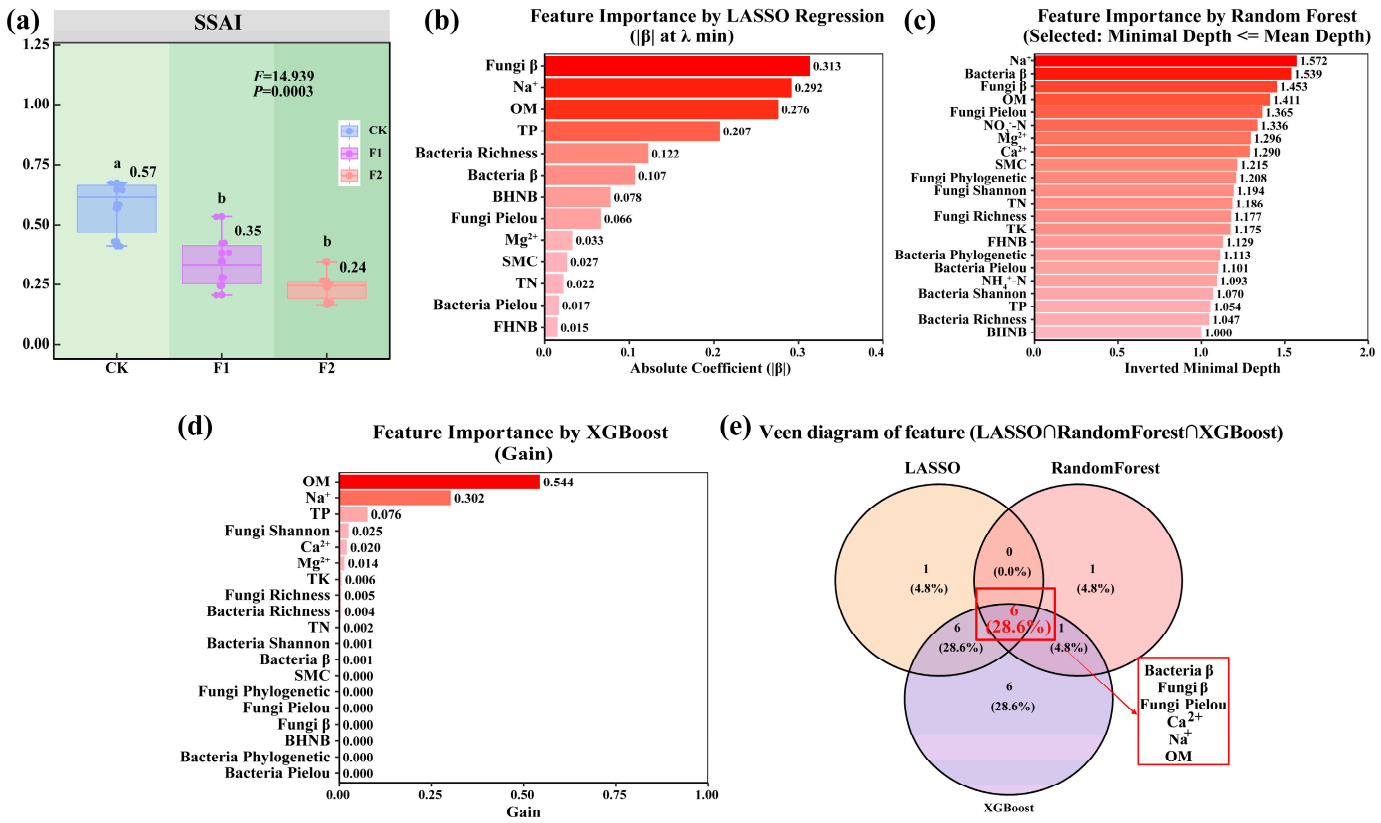


Figure 10. Effects of potassium fulvate on soil salinity–alkalinity and identification of key predictive factors using machine learning. (**a**) Soil Salinization and Alkalization Index (SSAI); (**b**) feature importance ranked by LASSO regression; (**c**) feature importance ranked by Random Forest; (**d**) feature importance ranked by XGBoost; (**e**) Venn diagram showing shared key predictors identified by LASSO, Random Forest, and XGBoost. Note: Different lowercase letters indicate significant differences among treatments. Soil Salinization and Alkalization Index (SSAI); organic matter (OM); total phosphorus (TP); total potassium (TK); total nitrogen (TN); nitrate nitrogen (NO_3^-–N); ammonium nitrogen (NH_4^+–N); soil moisture content (SMC); Bacteria Habitat Niche Breadth (BHNB); Fungi Habitat Niche Breadth (FHNB).

PF application exerted significant positive effects on both microbial communities (path coefficient = 0.89, $p < 0.001$) and soil properties (path coefficient = 0.93, $p < 0.001$; Figure 11a). Among these, soil factors, including organic matter (OM) and sodium ions (Na^+), had a significant direct negative impact on SSAI (path coefficient = −0.77, $p < 0.001$; Figure 11a), underscoring their central role in mitigating rhizospheric salinity–alkalinity stress. Despite the lack of a significant direct effect from microbial communities (path coefficient = −0.22), the decomposition of effects (Figure 11b) indicated that PF had the strongest overall negative effect on SSAI (−0.91), which was entirely mediated through indirect interactions involving microbial and soil factors.

Among all the factors tested, only the soil variables showed a direct and significant effect on the reduction in SSAI (−0.77) and functioned as the primary conduit in the PF-mediated regulatory pathway. Although microbial communities lacked direct effects, they played a mediating role in the PF-induced modulation of soil salinity–alkalinity stress.

In summary, rhizospheric soil salinization–alkalization was significantly and indirectly alleviated by PF through coordinated shifts in microbial community structure and soil characteristics. Soil properties acted as the core mediators, while microbial communities provided synergistic support in this mitigation process.

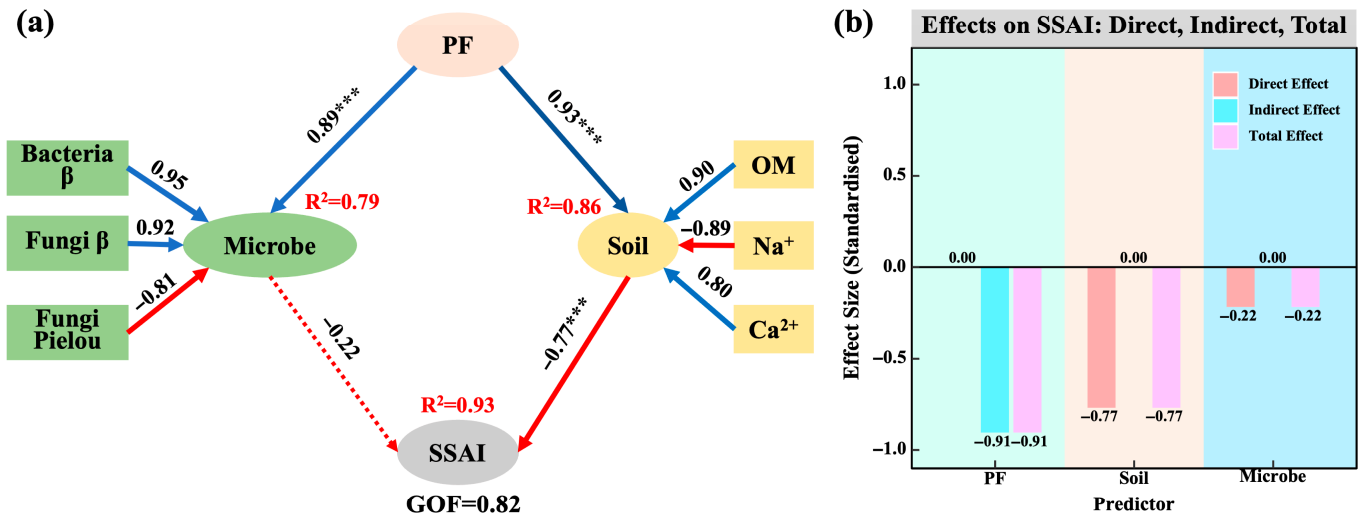


Figure 11. Pathways driven by potassium fulvate mitigating soil salinization and alkalization. (**a**) Partial least squares structural equation model (PLS-SEM) illustrating the direct and indirect links among potassium fulvate (PF), soil physicochemical properties, microbial communities, and the Soil Salinization and Alkalization Index (SSAI). (**b**) Decomposition of the direct, indirect, and total effects of PF, soil properties, and microbial communities on SSAI, quantified from the PLS-SEM. Note: Standardized path coefficients are shown adjacent to each arrow; blue arrows denote positive effects, red arrows negative effects, and arrow thickness is proportional to effect size. Solid arrows represent statistically significant paths, whereas dashed arrows indicate non-significant relationships. *** $p < 0.001$.

4. Discussion

4.1. Potassium Fulvate Promotes Plant Growth and Optimizes Rhizospheric Soil

The results demonstrated that potassium fulvate (PF) markedly enhanced oat growth under saline–alkaline stress ($p < 0.01$), with the most pronounced increases in both aboveground and belowground biomass observed under the higher application rate of 150 kg·hm^{-2} (F2). Plants receiving the F2 treatment demonstrated enhanced biomass production. Enhanced root surface area and volume indicated that PF improved root architecture, expanding the interface for water and nutrient uptake and thereby supporting accelerated shoot development. This observation is consistent with previous findings that fulvic acids enhance plant height and root development, ultimately increasing yield [60], and further confirms their function in promoting growth under saline–alkaline conditions [61].

In the rhizosphere, PF improved organic matter (OM), nitrate nitrogen (NO_3^-–N), and total potassium (TK), with the F2 treatment showing the most substantial enhancement ($p < 0.01$; Figure 4a,d,f). The increase in OM provided substrates for microbial communities and facilitated the chelation of salt ions, thereby indirectly mitigating saline–alkaline stress [23]. Enhanced potassium availability contributed to osmotic regulation and photosynthetic efficiency, both essential under salt stress conditions [25].

More importantly, PF conferred distinct benefits in modulating the ionic environment of the rhizosphere. In particular, the F2 treatment significantly reduced Na^+ concentration and the sodium adsorption ratio (SAR) ($p < 0.01$), effectively inhibiting the accumulation of stress-inducing alkaline ions [62,63]. Concurrently, PF application led to significant increases in Ca^{2+} concentrations and soil moisture content ($p < 0.05$), both of which may enhance soil aggregate stability and buffering capacity, thereby improving overall soil structure [64–66]. This ion exchange-based mechanism is supported by previous studies showing that Ca^{2+} replaces Na^+ via cation exchange, increases soil cation exchange capacity (CEC), and promotes aggregation, thereby alleviating alkalization [66]. In addition, PF

enhanced soil moisture content, highlighting its contribution to improving soil water-holding capacity ($p < 0.001$). These effects are consistent with the established roles of organic acid-based amendments in modulating soil pH and retaining moisture, both of which enhance soil buffering capacity and ionic stability [64,67].

4.2. Potassium Fulvate Alters Community Turnover and Reshapes Microbial Community Structure

Source–sink analysis provided additional insights into the directionality and extent of microbial community turnover. In bacterial communities, the dominant taxa remained stable following PF application, suggesting limited influence of environmental filtering on bacterial composition. In contrast, fungal communities under the F2 treatment underwent pronounced shifts, with reduced source contributions and increased endogenous replacement, indicating strong selective pressure and restructuring induced by PF. This response likely reflects the inherent sensitivity of fungal taxa to soil pH, carbon-to-nitrogen ratio, and moisture conditions [68,69]. By modulating these key physicochemical parameters, PF shifted fungal ecological niches (Figure 8), thereby promoting structural reorganization (Figure 7). These findings are consistent with the well-documented responsiveness of fungal communities to environmental shifts driven by organic amendments [70,71].

Bacterial α-diversity was largely unaffected by PF application, as diversity metrics did not differ significantly across treatments. This implies a degree of resistance in bacterial communities to exogenous organic inputs, potentially due to their high metabolic diversity and ecological redundancy [23]. In contrast, fungal α-diversity significantly declined under the F2 treatment ($p < 0.05$). This pattern aligns with the source-tracking analysis, which revealed a more pronounced decline in fungal contributions from the control (CK) than in bacterial ones.

4.3. Construction of the Salinization–Alkalization Stress Index (SSAI) and Its Ecological Regulation Pathways

Further elucidation of the mechanism by which potassium fulvate (PF) alleviates saline–alkaline stress was achieved through the development of a comprehensive Soil Salinization and Alkalization Index (SSAI), derived from three key indicators: sodium adsorption ratio (SAR), pH, and electrical conductivity (EC). In comparison with conventional single-parameter indices, SSAI demonstrates greater sensitivity and integrative capacity, providing a more reliable representation of soil salinity–alkalinity levels [72,73]. The experimental results demonstrated that PF application significantly reduced SSAI values ($p < 0.001$), with the most pronounced effect observed under the F2 treatment, thereby underscoring its potential for the system-level mitigation of saline–alkaline stress.

Identification of key determinants of SSAI variation was conducted using three machine learning models, namely LASSO regression, random forest, and XGBoost. Six variables, namely bacterial β-diversity, fungal β-diversity, fungal Pielou evenness, organic matter (OM), Na^+, and Ca^{2+}, were consistently identified across all models as robust predictors, reinforcing their cross-model reliability [57,74]. These findings suggest that rhizosphere microbial β-diversity, which reflects spatial heterogeneity in community composition, serves as a critical determinant of stress regulation, surpassing traditional α-diversity metrics in predictive capability [75–77]. Additionally, organic matter and ionic balance, characterized by reduced Na^+ and increased Ca^{2+} concentrations, emerged as primary regulators of saline–alkaline stress, indicating that soil salinity is dynamically modulated by organic matter inputs and cation composition [78–80].

The structural equation model clarified the statistical pathways through which PF-induced shifts in soil chemistry and microbial communities are associated with reduced salinity–alkalinity stress, offering quantitative support. The model indicated that PF

exerted no direct effect on SSAI; instead, its influence was entirely mediated through two indirect pathways involving microbial communities and soil properties. Among these, soil factors functioned as the principal mediators, exhibiting the only significant direct negative path coefficient (-0.77; $p < 0.001$), which underscores the dominant role of OM regulation and cation exchange capacity [81]. Although microbial communities exhibited no direct significant effect on SSAI ($p > 0.05$), they acted as important intermediaries. Notably, β-diversity played a critical role in shaping resource distribution and maintaining community functional stability [62,76,77].

In summary, PF alleviates rhizospheric saline–alkaline stress through coordinated soil–microbe interactions, conferring benefits that extend beyond simple nutrient supplementation. Although these short-term effects have clear agronomic value, their efficacy in the long-term rehabilitation of saline–alkaline soils remains to be verified. Even so, the present findings broaden the theoretical framework of saline-soil amelioration and offer new perspectives for the sustainable management of these fragile ecosystems.

5. Conclusions

In conclusion, potassium fulvate (PF) significantly enhances oat biomass, especially at the high application rate of 150 kg hm^{-2}. PF application improves soil fertility and optimizes the rhizospheric ionic environment by reducing sodicity indicators (Na^+, SAR), increasing beneficial ions (Ca^{2+}), and enhancing soil moisture content, thereby alleviating saline–alkaline stress. Fungal communities demonstrate greater sensitivity to PF than bacterial communities, exhibiting marked shifts in structure and diversity under high-dose treatments. By integrating machine learning approaches with structural equation modeling (SEM), we identified key determinants of the Soil Salinization and Alkalization Index (SSAI), highlighting the mediating role of microbial communities and the direct influence of soil physicochemical properties. This study demonstrates that potassium fulvate functions as an effective ecological regulator in saline–alkaline agro-systems, providing concrete strategies for soil amendment and crop management, and thus supporting sustainable agriculture in the saline–alkaline soils of the Qinghai–Tibet Plateau.

Supplementary Materials: The following supporting information can be downloaded at https://www.mdpi.com/article/10.3390/agronomy15071673/s1: Figure S1: Diagnostic plots for multi-algorithm feature selection in SSAI prediction.

Author Contributions: Conceptualization, J.W.; methodology, J.W.; software, J.W.; validation, X.J., J.W.; formal analysis, J.W.; investigation, X.L., Y.F., K.B., Z.Q., C.X. and W.W.; resources, J.W. and X.J.; data curation, J.W.; writing—original draft preparation, J.W.; writing—review and editing, J.W.; visualization, X.J.; supervision, J.W. and X.J.; project administration, J.W. and X.J.; funding acquisition, G.L. and H.Z. All authors have read and agreed to the published version of the manuscript.

Funding: This research was funded by National Natural Science Foundation of China Regional Innovation Development Joint Fund Project, "The rhizosphere synthetic microbiota promote vegetation restoration of saline soils in Qaidam Basin: the process, mechanism and method" (U23A2043).

Data Availability Statement: The data is deposited in the National Microbiology Data Center (NMDC) with the accession number NMDC10019863 (https://nmdc.cn/resource/genomics/project/detail/NMDC10019863, accessed on 1 July 2025).

Conflicts of Interest: Authors Yunjie Fu, Kui Bao and Zhixiu Quan were employed by the company Qinghai Bensheng Grass Industry Co., Ltd. The remaining authors declare that the research was conducted in the absence of any commercial or financial relationships that could be construed as a potential conflict of interest.

References

1. Shang, X.; Geng, L.; Yang, J.; Zhang, Y.; Xu, W. Transcriptome Analysis Reveals the Mechanism of Alkalinity Exposure on Spleen Oxidative Stress, Inflammation and Immune Function of *Luciobarbus capito*. *Ecotoxicol. Environ. Saf.* **2021**, *225*, 112748. [CrossRef] [PubMed]
2. Osakabe, Y.; Kawaoka, A.; Nishikubo, N.; Osakabe, K. Responses to Environmental Stresses in Woody Plants: Key to Survive and Longevity. *J. Plant Res.* **2012**, *125*, 1–10. [CrossRef]
3. Li, L.; Liu, H.; He, X.; Lin, E.; Yang, G. Winter Irrigation Effects on Soil Moisture, Temperature and Salinity, and on Cotton Growth in Salinized Fields in Northern Xinjiang, China. *Sustainability* **2020**, *12*, 7573. [CrossRef]
4. Zhang, Y.; Hou, K.; Qian, H.; Gao, Y.; Fang, Y.; Xiao, S.; Tang, S.; Zhang, Q.; Qu, W.; Ren, W. Characterization of Soil Salinization and Its Driving Factors in a Typical Irrigation Area of Northwest China. *Sci. Total Environ.* **2022**, *837*, 155808. [CrossRef] [PubMed]
5. Zhao, Y.; Chen, H.; Sun, H.; Yang, F. In the Qaidam Basin, Soil Nutrients Directly or Indirectly Affect Desert Ecosystem Stability under Drought Stress through Plant Nutrients. *Plants* **2024**, *13*, 1849. [CrossRef]
6. Yang, L.; Zhao, G.; Mu, X.; Lan, Z.; Jiao, J.; An, S.; Wu, Y.; Miping, P. Integrated Assessments of Land Degradation on the Qinghai-Tibet Plateau. *Ecol. Indic.* **2023**, *147*, 109945. [CrossRef]
7. Cuevas, J.; Daliakopoulos, I.N.; del Moral, F.; Hueso, J.J.; Tsanis, I.K. A Review of Soil-Improving Cropping Systems for Soil Salinization. *Agronomy* **2019**, *9*, 295. [CrossRef]
8. Howe, C.W.; Goemans, C.; Howe, C.W.; Goemans, C. Water Transfers and Their Impacts: Lessons from Three Colorado Water Markets. *J. Am. Water Resour. Assoc.* **2003**, *39*, 1055–1065. [CrossRef]
9. Zhang, B.; Wang, N. Study on the Harm of Saline Alkali Land and Its Improvement Technology in China. *IOP Conf. Ser. Earth Environ. Sci.* **2021**, *692*, 42053. [CrossRef]
10. Guo, Y.; Wang, Q.; Zhao, X.; Li, Z.; Li, M.; Zhang, J.; Wei, K. Field Irrigation Using Magnetized Brackish Water Affects the Growth and Water Consumption of *Haloxylon ammodendron* Seedlings in an Arid Area. *Front. Plant Sci.* **2022**, *13*, 929021. [CrossRef]
11. Haddeland, I.; Heinke, J.; Biemans, H.; Eisner, S.; Flörke, M.; Hanasaki, N.; Konzmann, M.; Ludwig, F.; Masaki, Y.; Schewe, J.; et al. Global Water Resources Affected by Human Interventions and Climate Change. *Proc. Natl. Acad. Sci. USA* **2014**, *111*, 3251–3256. [CrossRef] [PubMed]
12. Wang, J.; Feng, W.; Zhang, H.; Sun, J.; Zhao, Q. Experimental Study on the Effect of Deep Pine Technology on Water and Salt Transport in Soda Saline Land. *Arab. J. Geosci.* **2021**, *14*, 571. [CrossRef]
13. Wang, Y.; Hu, C.; Jia, X.; Ma, Q. Characteristics of Evapotranspiration and Water Consumption of Different Underlying Surfaces in Qaidam Basin. *Water* **2022**, *14*, 3469. [CrossRef]
14. Hui, R.; Tan, H. Divergence of Nutrients, Salt Accumulation, Bacterial Community Structure and Diversity in Soil after 8 Years of Flood Irrigation with Surface Water and Groundwater. *BMC Microbiol.* **2024**, *24*, 477. [CrossRef] [PubMed]
15. Xu, X.; Guo, L.; Wang, S.; Wang, X.; Ren, M.; Zhao, P.; Huang, Z.; Jia, H.; Wang, J.; Lin, A. Effective Strategies for Reclamation of Saline-Alkali Soil and Response Mechanisms of the Soil-Plant System. *Sci. Total Environ.* **2023**, *905*, 167179. [CrossRef] [PubMed]
16. Li, F.; Guo, Y.; Wang, Z.; Mu, Y. Influence of Different Phytoremediation on Soil Microbial Diversity and Community Composition in Saline-Alkaline Land. *Int. J. Phytorem.* **2022**, *24*, 507–517. [CrossRef]
17. Zhu, G.; Liu, J.; Wu, H.; Zhu, Y.; Nimir, N.E.A.; Zhou, G. The Optimum Mixed Cropping Ratio of Oat and Alfalfa Enhanced Plant Growth, Forage Yield, and Forage Quality in Saline Soil. *Plants* **2024**, *13*, 3103. [CrossRef]
18. Guo, C.; Xu, C.; Pu, X.; Zhao, Y.; Wang, J.; Fu, Y.; Wang, W. Oat and Forage Pea Mixed Sowing Improves Soil Chemical Fertility and Fresh and Dry Mass Yield in Light Saline–Alkali Land: Preliminary Results. *Agronomy* **2025**, *15*, 297. [CrossRef]
19. Wang, J.; Zhao, A.; Ma, F.; Liu, J.; Xiao, G.; Xu, X. Amendment of Saline–Alkaline Soil with Flue-Gas Desulfurization Gypsum in the Yinchuan Plain, Northwest China. *Sustainability* **2023**, *15*, 8658. [CrossRef]
20. Xiao, F.; Zhou, B.; Wang, H.; Duan, M.; Feng, L. Effects of Different Soil Amendments on Physicochemical Property of Soda Saline-Alkali Soil and Crop Yield in Northeast China. *Int. J. Agric. Biol. Eng.* **2022**, *15*, 192–198. [CrossRef]
21. Zhou, M.; Liu, X.; Meng, Q.; Zeng, X.; Zhang, J.; Li, D.; Wang, J.; Du, W.; Ma, X. Additional Application of Aluminum Sulfate with Different Fertilizers Ameliorates Saline-Sodic Soil of Songnen Plain in Northeast China. *J. Soils Sediments* **2019**, *19*, 3521–3533. [CrossRef]
22. Alsudays, I.M.; Alshammary, F.H.; Alabdallah, N.M.; Alatawi, A.; Alotaibi, M.M.; Alwutayd, K.M.; Alharbi, M.M.; Alghanem, S.M.S.; Alzuaibr, F.M.; Gharib, H.S.; et al. Applications of Humic and Fulvic Acid under Saline Soil Conditions to Improve Growth and Yield in Barley. *BMC Plant Biol.* **2024**, *24*, 191. [CrossRef]
23. Jiao, Y.; Chen, Q.; Guo, X.; Li, H.; Chen, X.; Men, K.; Liu, X.; Shang, X.; Gao, Y.; Zhang, L.; et al. Effect of Potassium Fulvate on Continuous Tobacco Cropping Soils and Crop Growth. *Front. Plant Sci.* **2024**, *15*, 1457793. [CrossRef]
24. Sun, Y.; Yang, J.; Yao, R.; Chen, X.; Wang, X. Biochar and Fulvic Acid Amendments Mitigate Negative Effects of Coastal Saline Soil and Improve Crop Yields in a Three Year Field Trial. *Sci. Rep.* **2020**, *10*, 8946. [CrossRef]

25. El-Shaboury, H.; Baddour, A.G.A. Effects of Various Organic Fertilizer Sources and External Applications of Potassium Fulvate and Potassium Citrate on the Yield and Quality of Two Barley Varieties Grown under Salt Affected Soil. *J. Soil Sci. Agric. Eng.* **2024**, *15*, 117–123. [CrossRef]
26. Lumactud, R.A.; Gorim, L.Y.; Thilakarathna, M.S. Impacts of Humic-Based Products on the Microbial Community Structure and Functions toward Sustainable Agriculture. *Front. Sustain. Food Syst.* **2022**, *6*, 977121. [CrossRef]
27. Whitton, M.M.; Ren, X.; Yu, S.J.; Irving, A.D.; Trotter, T.; Bajagai, Y.S.; Stanley, D. Humate Application Alters Microbiota–Mineral Interactions and Assists in Pasture Dieback Recovery. *Heliyon* **2023**, *9*, e13327. [CrossRef]
28. Zeng, F.; Zhang, X.; Zhan, T.; Zhang, Z.; Chen, L.; Chen, L.; Ji, M. Rapid Warming and Increasing Moisture Levels in the Qaidam Basin. *Theor. Appl. Climatol.* **2024**, *155*, 7121–7132. [CrossRef]
29. Lin, X.; Pan, S.; Zhang, W.; Jia, X.; Chen, X.; An, K.; Wu, L.; Huang, J.; Chen, X.; Chen, H. Establishing the Modern-like Differential Climate of the Qaidam Basin, Northeast Tibetan Plateau, since ca. 9 Ma: Implications of the Effect of Interactions between Tectonics and Atmospheric Circles on Paleoclimate. *GSA Bull.* **2024**, *137*, 2258–2270. [CrossRef]
30. Shi, X.Z.; Yu, D.S.; Warner, E.D.; Pan, X.Z.; Petersen, G.W.; Weindorf, D.C. Soil Database of 1:1,000,000 Digital Soil Survey and Reference System of the Chinese Genetic Soil Classification System. *Soil Surv. Horiz.* **2004**, *45*, 129–136. [CrossRef]
31. IUSS Working Group WRB. *World Reference Base for Soil Resources: International Soil Classification System for Naming Soils and Creating Legends for Soil Maps*, 4th ed.; International Union of Soil Sciences (IUSS): Vienna, Austria, 2022; ISBN 979-8-9862451-1-9.
32. Richards, L.A. Diagnosis and Improvement of Saline and Alkali Soils. *Soil Sci.* **1954**, *78*, 154. [CrossRef]
33. Paz, A.M.; Amezketa, E.; Canfora, L.; Castanheira, N.; Falsone, G.; Goncalves, M.C.; Gould, I.; Hristov, B.; Mastrorilli, M.; Ramos, T.; et al. Salt-Affected Soils: Field-Scale Strategies for Prevention, Mitigation, and Adaptation to Salt Accumulation. *Ital. J. Agron.* **2023**, *18*, 2166. [CrossRef]
34. Liu, L.; Zhu, N.; Zhou, G.; Dang, P.; Yang, X.; Qiu, L.; Huang, M.; Gong, Y.; Zhao, S.; Chen, J. Response of Soil Microbial Community to Plant Composition Changes in Broad-Leaved Forests of the Karst Area in Mid-Subtropical China. *PeerJ* **2022**, *10*, e12739. [CrossRef]
35. Zhu, G.; Schmidt, O.; Luan, L.; Xue, J.; Fan, J.; Geisen, S.; Sun, B.; Jiang, Y. Bacterial Keystone Taxa Regulate Carbon Metabolism in the Earthworm Gut. *Microbiol. Spectr.* **2022**, *10*, e0108122. [CrossRef]
36. Zhao, Y.; Wang, Y.; Sun, S.; Liu, W.; Zhu, L.; Yan, X. Different Forms and Proportions of Exogenous Nitrogen Promote the Growth of Alfalfa by Increasing Soil Enzyme Activity. *Plants* **2022**, *11*, 1057. [CrossRef] [PubMed]
37. Bai, Y.; Qin, Y.; Lu, X.; Zhang, J.; Chen, G.; Li, X. Fractal Dimension of Particle-Size Distribution and Their Relationships with Alkalinity Properties of Soils in the Western Songnen Plain, China. *Sci. Rep.* **2020**, *10*, 20603. [CrossRef]
38. He, Y.; Liu, X.; Lv, Y.; Liu, F.; Peng, J.; Shen, T.; Zhao, Y.; Tang, Y.; Luo, S. Quantitative Analysis of Nutrient Elements in Soil Using Single and Double-Pulse Laser-Induced Breakdown Spectroscopy. *Sensors* **2018**, *18*, 1526. [CrossRef]
39. Bi, B.; Wang, K.; Zhang, H.; Wang, Y.; Fei, H.; Pan, R.; Han, F. Plants Use Rhizosphere Metabolites to Regulate Soil Microbial Diversity. *Land Degrad. Dev.* **2021**, *32*, 5267–5280. [CrossRef]
40. Ciccazzo, S.; Esposito, A.; Rolli, E.; Zerbe, S.; Daffonchio, D.; Brusetti, L. Safe-Site Effects on Rhizosphere Bacterial Communities in a High-Altitude Alpine Environment. *Biomed. Res. Int.* **2014**, *2014*, 480170. [CrossRef]
41. Schmidt Jennifer, E.; Vannette Rachel, L.; Igwe, A.; Blundell, R.; Casteel Clare, L.; Gaudin Amélie, C.M. Effects of Agricultural Management on Rhizosphere Microbial Structure and Function in Processing Tomato Plants. *Appl. Environ. Microbiol.* **2019**, *85*, e01064-19. [CrossRef]
42. Shenhav, L.; Thompson, M.; Joseph, T.A.; Briscoe, L.; Furman, O.; Bogumil, D.; Mizrahi, I.; Pe'er, I.; Halperin, E. FEAST: Fast Expectation-Maximization for Microbial Source Tracking. *Nat. Methods* **2019**, *16*, 627–632. [CrossRef] [PubMed]
43. Faith, D.P. Conservation Evaluation and Phylogenetic Diversity. *Biol. Conserv.* **1992**, *61*, 1–10. [CrossRef]
44. Dixon, P. VEGAN, a Package of R Functions for Community Ecology. *J. Veg. Sci.* **2003**, *14*, 927–930. [CrossRef]
45. Thévenot, E.A.; Roux, A.; Xu, Y.; Ezan, E.; Junot, C. Analysis of the Human Adult Urinary Metabolome Variations with Age, Body Mass Index, and Gender by Implementing a Comprehensive Workflow for Univariate and OPLS Statistical Analyses. *J. Proteome Res.* **2015**, *14*, 3322–3335. [CrossRef]
46. Anderson, M.J. A New Method for Non-Parametric Multivariate Analysis of Variance. *Austral Ecol.* **2001**, *26*, 32–46. [CrossRef]
47. Wang, Y.; Li, R.; Wu, X.; Yan, Y.; Wei, C.; Luo, M.; Xiao, Y.; Zhang, Y. Evaluation of Groundwater Quality for Drinking and Irrigation Purposes Using GIS-Based IWQI, EWQI and HHR Model. *Water* **2023**, *15*, 2233. [CrossRef]
48. Khan, M.H.; Xiao, Y.; Yang, H.; Zhang, Y.; Wang, L.; Wang, J.; Hu, W.; Chen, F.; Shrestha, R. Geochemical Characteristics, Mechanisms, and Suitability of Groundwater Resource for Sustainable Water Supply in Quetta Valley. *Water Supply* **2024**, *24*, 1802–1824. [CrossRef]
49. Kreyling, J.; Jentsch, A.; Beier, C. Beyond Realism in Climate Change Experiments: Gradient Approaches Identify Thresholds and Tipping Points. *Ecol. Lett.* **2014**, *17*, 125-e1. [CrossRef]

50. Maestre, F.T.; Quero, J.L.; Gotelli, N.J.; Escudero, A.; Ochoa, V.; Delgado-Baquerizo, M.; García-Gómez, M.; Bowker, M.A.; Soliveres, S.; Escolar, C.; et al. Plant Species Richness and Ecosystem Multifunctionality in Global Drylands. *Science* **2012**, *335*, 214–218. [CrossRef]
51. Li, H.; Zhou, X.; Huang, K.; Hao, G.; Li, J. Research on Optimal Control of Non-Point Source Pollution: A Case Study from the Danjiang River Basin in China. *Environ. Sci. Pollut. Res.* **2022**, *29*, 15582–15602. [CrossRef]
52. Bhatt, A.G.; Kumar, A.; Trivedi, P.R. Integration of Multivariate Statistics and Water Quality Indices to Evaluate Groundwater Quality and Its Suitability in Middle Gangetic Floodplain, Bihar. *SN Appl. Sci.* **2021**, *3*, 426. [CrossRef]
53. Basu, S.; Kumbier, K.; Brown, J.B.; Yu, B. Iterative Random Forests to Discover Predictive and Stable High-Order Interactions. *Proc. Natl. Acad. Sci. USA* **2018**, *115*, 1943–1948. [CrossRef]
54. Shi, Y.; Fang, J.; Li, J.; Yu, K.; Zhu, J.; Lu, Y. Fracture Risk Prediction in Diabetes Patients Based on Lasso Feature Selection and Machine Learning. *Comput. Methods Biomech. Biomed. Eng.* **2024**. [CrossRef] [PubMed]
55. Yu, F.; Wei, C.; Deng, P.; Peng, T.; Hu, X. Deep Exploration of Random Forest Model Boosts the Interpretability of Machine Learning Studies of Complicated Immune Responses and Lung Burden of Nanoparticles. *Sci. Adv.* **2021**, *7*, eabf4130. [CrossRef]
56. Lin, X.; Gao, F.; Lin, H.; Yao, W.; Wang, Y. XGBoost-Based Nomogram for Predicting Lymph Node Metastasis in Endometrial Carcinoma. *Am. J. Cancer Res.* **2024**, *14*, 5769–5783. [CrossRef] [PubMed]
57. Zhang, Z.; Zhang, Q.; Chen, B.; Yu, Y.; Wang, T.; Xu, N.; Fan, X.; Penuelas, J.; Fu, Z.; Deng, Y.; et al. Global Biogeography of Microbes Driving Ocean Ecological Status under Climate Change. *Nat. Commun.* **2024**, *15*, 4657. [CrossRef]
58. Lu, M.; He, G.; Fan, L.; Liu, G.; Wu, J.; Liu, W.; Ma, L. Temperature Sensitivity of Aerobic and Anaerobic Organic Carbon Mineralization Varies with Climate and Soil Depth in Riparian Zones. *Soil Biol. Biochem.* **2024**, *195*, 109455. [CrossRef]
59. Tan, Y.; Wang, Z. Research on Influencing Factors of Soybean Yield in China's Northeast Black Soil Region Based on PLS-SEM. *Front. Sustain. Food Syst.* **2024**, *8*, 1436224. [CrossRef]
60. Mosaad, I.S.M.; Selim, E.-M.M.; Gaafar, D.E.M.; Al-Anoos, M.A.T. Effects of Humic and Fulvic Acids on Forage Production and Grain Quality of Triticale under Various Soil Salinity Levels. *Cereal Res. Commun.* **2024**. [CrossRef]
61. Abbas, G.; Rehman, S.; Siddiqui, M.H.; Ali, H.M.; Farooq, M.A.; Chen, Y. Potassium and Humic Acid Synergistically Increase Salt Tolerance and Nutrient Uptake in Contrasting Wheat Genotypes through Ionic Homeostasis and Activation of Antioxidant Enzymes. *Plants* **2022**, *11*, 263. [CrossRef]
62. Zhang, M.; Li, X.; Wang, X.; Feng, J.; Zhu, S. Potassium Fulvic Acid Alleviates Salt Stress of Citrus by Regulating Rhizosphere Microbial Community, Osmotic Substances and Enzyme Activities. *Front. Plant Sci.* **2023**, *14*, 1161469. [CrossRef] [PubMed]
63. Ren, M.; Mao, G.; Zheng, H.; Wang, W.; Tang, Q. Growth Changes of Tomato Seedlings Responding to Sodium Salt of α-Naphthalene Acetic Acid and Potassium Salt of Fulvic Acid. *Sci. Rep.* **2023**, *13*, 4024. [CrossRef]
64. Fan, J.; Lv, Q.; Zhou, T.; Wang, T.; Gao, H.; Zhou, W.; Ren, X.; Hu, S. Calcium Lactate as a Soil Amendment: Mechanistic Insights into Its Effect on Salinity, Alkalinity, and Aggregation in Saline-Alkaline Soils. *Soil Tillage Res.* **2025**, *248*, 106459. [CrossRef]
65. Zhu, Y.; Ali, A.; Dang, A.; Wandel, A.P.; Bennett, J.M. Re-Examining the Flocculating Power of Sodium, Potassium, Magnesium and Calcium for a Broad Range of Soils. *Geoderma* **2019**, *352*, 422–428. [CrossRef]
66. El-Kamar, F. Effect of Humic Acid and Yeast Waste Application on Fababean (*Vicia faba*) Yield, Yield Components and Some Soil Properties of Salt Affected Soil. *J. Soil Sci. Agric. Eng.* **2020**, *11*, 483–488. [CrossRef]
67. Song, H.; Nam, K. Development of a Potassium-Based Soil Washing Solution Using Response Surface Methodology for Efficient Removal of Cesium Contamination in Soil. *Chemosphere* **2023**, *332*, 138854. [CrossRef]
68. Canini, F.; Zucconi, L.; Pacelli, C.; Selbmann, L.; Onofri, S.; Geml, J. Vegetation, pH and Water Content as Main Factors for Shaping Fungal Richness, Community Composition and Functional Guilds Distribution in Soils of Western Greenland. *Front. Microbiol.* **2019**, *10*, 2348. [CrossRef]
69. Yao, R.; Yang, J.; Zhu, W.; Li, H.; Yin, C.; Jing, Y.; Wang, X.; Xie, W.; Zhang, X. Impact of Crop Cultivation, Nitrogen and Fulvic Acid on Soil Fungal Community Structure in Salt-Affected Alluvial Fluvo-Aquic Soil. *Plant Soil* **2021**, *464*, 539–558. [CrossRef]
70. Glassman, S.I.; Wang, I.J.; Bruns, T.D. Environmental Filtering by pH and Soil Nutrients Drives Community Assembly in Fungi at Fine Spatial Scales. *Mol. Ecol.* **2017**, *26*, 6960–6973. [CrossRef]
71. Kivlin, S.N.; Winston, G.C.; Goulden, M.L.; Treseder, K.K. Environmental Filtering Affects Soil Fungal Community Composition More than Dispersal Limitation at Regional Scales. *Fungal Ecol.* **2014**, *12*, 14–25. [CrossRef]
72. Li, H.; Wang, B.; Siri, M.; Liu, C.; Feng, C.; Shao, X.; Liu, K. Calcium-Modified Biochar Rather than Original Biochar Decreases Salinization Indexes of Saline-Alkaline Soil. *Environ. Sci. Pollut. Res.* **2023**, *30*, 74966–74976. [CrossRef] [PubMed]
73. Sarani, F.; Ahangar, A.G.; Shabani, A. Predicting ESP and SAR by Artificial Neural Network and Regression Models Using Soil pH and EC Data (Miankangi Region, Sistan and Baluchestan Province, Iran). *Arch. Agron. Soil Sci.* **2016**, *62*, 127–138. [CrossRef]
74. Zhang, Z.; Chi, Y.; Fu, Z.; Li, T.; Hu, R.; Zhang, Y.; Lu, Z.; Sun, J. Indirect Prediction Based on Machine Learning and Remote Sensing of Ecological Stoichiometric Ratio Superior to Direct Prediction. *Land Degrad. Dev.* **2025**. [CrossRef]

75. Yang, X.; Dai, Z.; Yuan, R.; Guo, Z.; Xi, H.; He, Z.; Wei, M. Effects of Salinity on Assembly Characteristics and Function of Microbial Communities in the Phyllosphere and Rhizosphere of Salt-Tolerant Avicennia Marina Mangrove Species. *Microbiol. Spectr.* **2023**, *11*, e03000–e03022. [CrossRef] [PubMed]
76. Fan, W.; Xiao, Y.; Dong, J.; Xing, J.; Tang, F.; Shi, F. Variety-Driven Rhizosphere Microbiome Bestows Differential Salt Tolerance to Alfalfa for Coping with Salinity Stress. *Front. Plant Sci.* **2023**, *14*, 1324333. [CrossRef]
77. Li, R.; Jiao, H.; Sun, B.; Song, M.; Yan, G.; Bai, Z.; Wang, J.; Zhuang, X.; Hu, Q. Understanding Salinity-Driven Modulation of Microbial Interactions: Rhizosphere versus Edaphic Microbiome Dynamics. *Microorganisms* **2024**, *12*, 683. [CrossRef]
78. Wang, S.; Gao, P.; Zhang, Q.; Shi, Y.; Guo, X.; Lv, Q.; Wu, W.; Zhang, X.; Li, M.; Meng, Q. Application of Biochar and Organic Fertilizer to Saline-Alkali Soil in the Yellow River Delta: Effects on Soil Water, Salinity, Nutrients, and Maize Yield. *Soil Use Manag.* **2022**, *38*, 1679–1692. [CrossRef]
79. Xie, Y.; Ning, H.; Zhang, X.; Zhou, W.; Xu, P.; Song, Y.; Li, N.; Wang, X.; Liu, H. Reducing the Sodium Adsorption Ratio Improves the Soil Aggregates and Organic Matter in Brackish-Water-Irrigated Cotton Fields. *Agronomy* **2024**, *14*, 2169. [CrossRef]
80. Liu, J.; Xie, W.; Yang, J.; Yao, R.; Wang, X.; Li, W. Effect of Different Fertilization Measures on Soil Salinity and Nutrients in Salt-Affected Soils. *Water* **2023**, *15*, 3274. [CrossRef]
81. Li, D.; Qiu, H.; Tian, G.; Zhao, Y.; Zhou, X.; He, S. Soil Salinity Is the Main Factor Influencing the Soil Bacterial Community Assembly Process under Long-Term Drip Irrigation in Xinjiang, China. *Front. Microbiol.* **2023**, *14*, 1291962. [CrossRef]

Disclaimer/Publisher's Note: The statements, opinions and data contained in all publications are solely those of the individual author(s) and contributor(s) and not of MDPI and/or the editor(s). MDPI and/or the editor(s) disclaim responsibility for any injury to people or property resulting from any ideas, methods, instructions or products referred to in the content.